

Supplementary material for
Broadband shifts in LFP power spectra are correlated with
single-neuron spiking in humans

Jeremy R. Manning¹, Joshua Jacobs², Itzhak Fried^{3,4}, and Michael J. Kahana²

¹Neuroscience Graduate Group and ²Department of Psychology, University of Pennsylvania,
Philadelphia, PA 19104

³Division of Neurosurgery and Semel Institute of Neuroscience and Human Behavior, University
of California, Los Angeles, CA 90095

⁴Functional neurosurgery unit, Tel-Aviv Medical Center and Sackler Faculty of Medicine,
Tel-Aviv University, Tel-Aviv 69978, Israel

Overview

This document is comprised of three main sections. First we include a supplementary figure illustrating each major component of the analysis framework used in “Broadband shifts in LFP power spectra are correlated with single-neuron spiking in humans.” In the second section we comment on the effect of the appearance of spike waveforms on the shape of the LFP power spectrum. Finally, we includes a table summarizing the number of broadband- and narrowband-shift neurons identified for each patient.

Supplemental Methods

Figure S1 illustrates the major components of the analysis we used to tag neurons as broadband- and narrowband-shift neurons. Synthetic data are shown in the figure in order to clearly illustrate the methods. As shown in Panel **a**, we first record a local field potential (Voltage, top sub-panel) and simultaneous spiking activity for nearby individual neurons (tick marks, bottom sub-panel). We then convolve the spike train with a Gaussian kernel to obtain a smoothed estimate of firing rate at each point in time during the recording session (Firing rate, bottom sub-panel). We next divide the recording session into 500 ms epochs. We thus obtain a distribution containing mean firing rates recorded during each epoch of the recording session. As shown in Panel **b**, we divide the distribution of firing rates into five equally spaced bins, such that each epoch is labeled according to its associated firing rate bin (indicated by different colors). We also compute mean LFP power spectra for each epoch. In Panel **c**, as in Figures 2, 3, 4, and 7 of the main text, the power spectra of epochs in each firing rate bin are averaged together and displayed using the same color scheme as in Panel **b**. We use robust regression (dotted lines) to capture the underlying $\frac{1}{f^a}$ shape of the power spectra while ignoring narrowband peaks. As shown, broadband power is equal to the mean height of the robust regression line. We also measure narrowband power by averaging the normalized power in each frequency band (see *Methods*). The panel shows that when the neuron’s firing rate increases, the LFP power spectrum exhibits an increase in broadband power coupled with a simultaneous decrease in power at a single narrow frequency band. In Panels **d** and **e**, each epoch is represented by a single dot. Note the overall positive relation between broadband power and firing rate illustrated in Panel **d**, and the overall negative relation between narrowband power and firing rate illustrated in Panel **e**. As illustrated in Panel **f**, we assess the degree to which broadband and narrowband power inform us about the neuron’s firing rate using a series of five least-squares regressions with broadband and narrowband power as regressors; each regression uses a different narrow frequency band. A neuron is tagged as a broadband-shift neuron if the β_B coefficients have the same sign and are significant in all five regressions. The neuron is tagged as a narrowband-shift neuron if only one β_F coefficient is significant, or if two β_f coefficients (corresponding to neighboring frequency bands) are significant and have the same sign. See *Methods* for details on the bootstrap procedure we used to determine the significance of each β coefficient in the regressions.

Supplemental Results

Effect of spike waveform shape on the LFP power spectrum. In extracellular recordings, the shape of action potentials resembles an impulse function, which has spectral power at a broad range of frequencies. We thus considered the possibility that our main finding of a positive

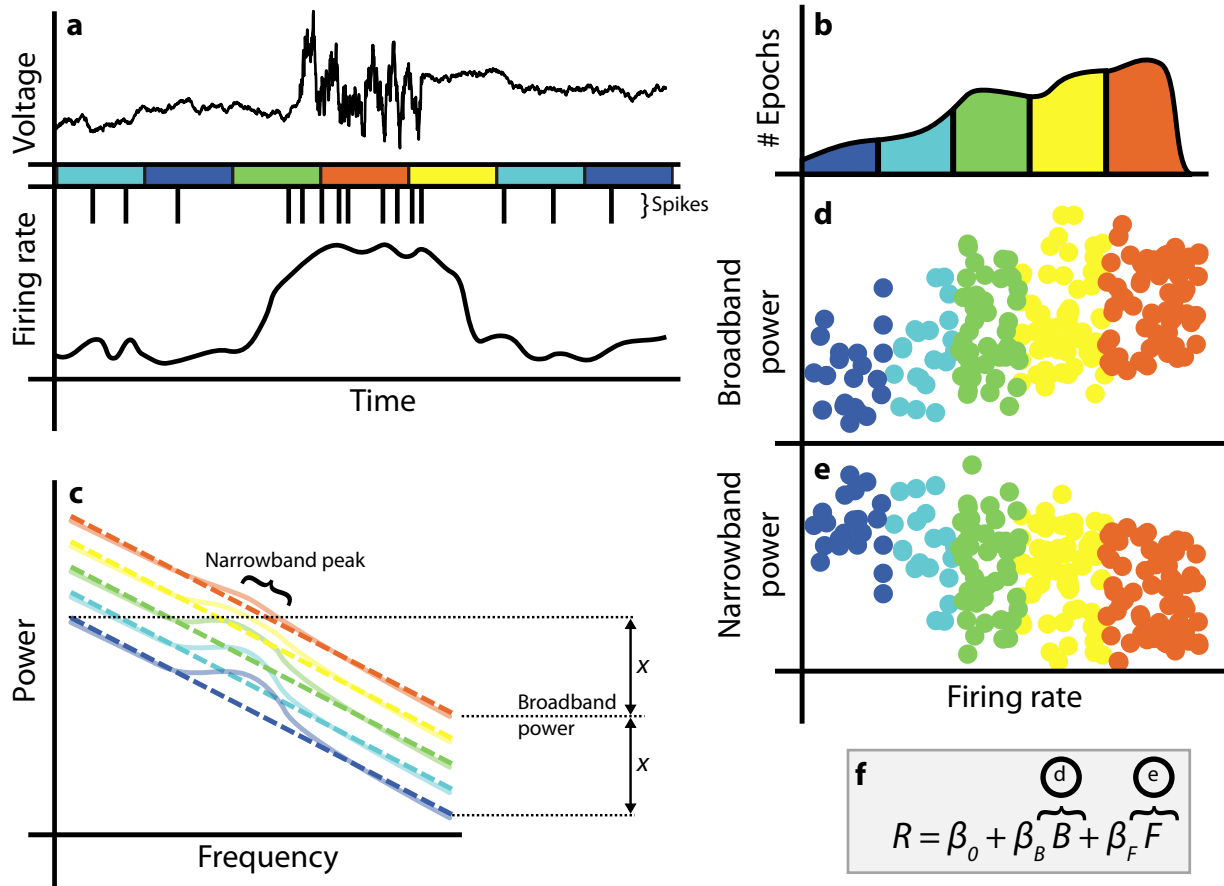


Figure S1: **Schematic of our analysis framework.** All panels contain synthetic data for illustrative purposes. **a.** This panel depicts the local field potential (Voltage, top sub-panel) and simultaneous spiking activity for nearby individual neurons (tick marks, bottom sub-panel). We convolve the spike train with a Gaussian kernel to obtain a smoothed estimate of firing rate at each point in time (Firing rate, bottom sub-panel). Rectangles are colored according to the firing rate of each epoch. **b.** This panel illustrates the distribution of mean firing rates recorded across all 500 ms epochs in the recording session. We divide the distribution of firing rates into 5 equally-spaced bins (indicated by different colors). **c.** Here we show mean power spectra for epochs in each firing rate bin (solid lines). We use robust regression (dotted lines) to capture the underlying $\frac{1}{f^\alpha}$ shape of the power spectra while ignoring narrowband peaks. We also measure narrowband power by averaging the normalized power in each frequency band (see *Methods*). **d,e.** These panels illustrate the relation between firing rate and broadband power (Panel d) or narrowband power in a single frequency band (Panel e). Each epoch is represented by a single dot in each panel. **f.** We use a series of least-squares regressions to determine whether the neuron is a broadband- and/or narrowband-shift neuron.

correlation between broadband power and neuronal spiking is a consequence of measuring action-potential waveforms. As described in *Methods*, we used a linear interpolation to remove each spike waveform from the LFP recording. However, it is possible that our cluster-cutting algorithm missed a number of spikes, and that that these unremoved spikes are responsible for the broadband shifts we observed in many neurons. To test this possibility, we re-ran our entire analysis without removing spike waveforms from the LFP. If our main effect had been driven by the appearance of spike waveforms in the LFP, then keeping spike waveforms in the LFP would be expected to

increase the magnitude of the broadband-shift effect. Instead, here we found that the number of neurons of positive broadband-shift neurons actually decreased (from 697 to 602), rather than increased, without spike removal. This suggests that the appearance of the spike waveform in the LFP does not account for the positive broadband shifts we observed.

Subject Table

Subject	Sessions	Observed Neurons	BB+	BB-	$\delta+$	$\delta-$	$\theta+$	$\theta-$	$\alpha+$	$\alpha-$	$\beta+$	$\beta-$	$\gamma+$	$\gamma-$
1	1	73	16	9	1	2	0	2	0	0	7	0	3	3
2	2	103	41	5	1	1	0	1	0	0	4	1	13	9
3	1	31	15	0	0	0	1	0	2	0	4	0	5	1
4	3	183	46	8	0	2	1	1	6	0	18	0	8	24
5	2	56	22	0	3	1	1	0	1	0	6	1	9	0
6	3	161	52	0	0	2	3	5	0	2	12	1	18	8
7	2	92	37	3	1	1	0	0	1	0	6	0	14	7
8	1	81	25	3	0	0	0	0	1	0	4	0	12	12
9	3	189	40	5	0	0	3	1	0	1	4	0	24	18
10	3	164	48	3	1	2	0	2	1	1	4	0	14	20
11	3	180	42	6	1	2	0	1	5	1	13	0	22	13
12	4	195	58	5	0	6	0	0	1	0	4	4	39	13
13	2	113	46	1	2	0	1	2	4	1	6	0	26	7
14	3	80	39	2	3	1	1	0	1	0	1	2	11	3
15	4	80	45	1	0	1	0	0	1	0	5	0	17	1
16	1	22	16	0	0	0	0	0	2	0	0	0	3	0
17	1	41	17	0	0	0	0	0	0	1	1	1	2	2
18	2	63	20	6	5	0	0	0	0	0	3	0	8	8
19	3	85	53	5	1	1	0	0	1	0	6	0	13	5
20	2	38	19	0	0	0	0	0	0	0	4	0	6	3
Total	46	2,030	697	62	19	22	11	15	27	7	112	10	267	157

Table S1: **Summary of observed neurons.** Columns 4 - 15 indicate, for each subject, the number of identified positive (+) and negative (-) broadband-shift neurons (BB), and for each frequency band (δ , θ , α , β , and γ) the number of narrowband-shift neurons. Each neuron appears in at most one broadband column (BB+ or BB-) and at most two narrowband columns of the same sign, for neighboring frequencies (e.g. $\beta+$ and $\gamma+$).